Available online at www.sciencedirect.com
ScienceDirect
Ceramics International 35 (2009) 213–220
CERAMICS INTERNATIONAL
www.elsevier.com/locate/ceramint

Preparation and characterization of ceramic composites derived from rice husk ash and polysiloxane

E.J. Siqueira [a], I.V.P. Yoshida [b], L.C. Pardini [c], M.A. Schiavon [a,*]

[a] Departamento de Ciências Naturais, Universidade Federal de São João Del Rei, 36301-160 São João Del Rei, MG, Brazil
[b] Instituto de Química, UNICAMP, CP 6154, 13083-970 Campinas, SP, Brazil
[c] Centro Técnico Aeroespacial, Divisão de Materiais, AMR, 12228-904 São José dos Campos, SP, Brazil

Received 19 July 2007; received in revised form 25 August 2007; accepted 3 October 2007
Available online 8 December 2007

Abstract

Ceramic matrix composites (CMCs) were prepared from a polysiloxane network filled with rice husk ash (RHA), a reactive filler. CMCs were obtained by pyrolysis at 1000 and 1600 °C of green bodies prepared from a mixture of polysiloxane network and RHA at a weight ratio of 4:1, respectively. The RHA and the CMCs were characterized by thermogravimetric analysis (TGA), X-ray diffraction (XRD), scanning electron microscopy (SEM) with energy-dispersive X-ray spectroscopy (EDS), in addition to density and mechanical measurements. The CMCs were obtained without macroscopic defects, and their initial observed porosity was reduced by polymeric infiltrations cycles of the polymeric precursor, which improved their flexural strength and modulus up to 100%.

Keywords: B. Composites; D. SiC; Ceramics; Polysiloxane; Rice husk ash

1. Introduction

The manufacture of ceramics derived from polymeric precursors has many advantages over the conventional method of ceramic preparation [1]. Among the variety of polymeric precursors, polysiloxanes are relatively cheap materials that have received special attention as precursors of silicon oxycarbide glasses [1,2]. Such glasses are constituted of random arrangement of tetra-coordinated silicon sites, whose general formula is $SiO_xC_{(4-x)}$, where $0 \leq x \leq 4$, or simply SiOC, and presents thermal and mechanical properties superior to the silica glasses [3–5].

The formation of bulk ceramics from polymer precursors, however, is difficult to achieve due to the high volume shrinkage associated with the polymer–ceramic conversion, which leads to intrinsic microcracks. In order to reduce the shrinkage upon pyrolysis, suitable filler materials can be incorporated into the polymeric precursors. Two types of fillers may be chosen: ''inactive fillers'', which remain inert during the pyrolysis, and ''active fillers'', which react with the pyrolysis by-products and/or gas of the atmosphere to form carbides or nitrides at high temperatures. The process associated with the incorporation of the latter is called AFCOP (active-filler-controlled polymer pyrolysis), and has been developed by Greil [6]. According to this approach, the polymer is partially filled with active powder particles, which after pyrolysis and under the appropriate conditions, generate reaction-bonded composite ceramics of variable compositions and high-dimensional stability. In the systems derived from inactive fillers, the intrinsic shrinkage and porosity formation during the polymer–ceramic conversion can be reduced, according to the filler volume effect [6,7]. Employing reactive filler particles, the reactions between these particles and the decomposition products of the polymeric phase or the reactive gas atmosphere promote a volume expansion. Consequently, near-net-shaped crack-free composites can be achieved, as the appropriate filler expansion compensates for the polymer shrinkage [6]. Combinations of different polymers, fillers, and reactive atmospheres may result in a variety of novel ceramic composite materials. Indeed, a number of systems have already been investigated using polysiloxanes as preceramic polymers filled with different ceramic [3] or metallic powders [6–8].

* Corresponding author. Tel.: +55 32 3379 2444; fax: +55 32 3379 2483.
E-mail address: schiavon@ufsj.edu.br (M.A. Schiavon).

0272-8842/$34.00
doi:10.1016/j.ceramint.2007.10.013

On the other hand, rice husk is an abundant material, produced in many countries around the world containing approximately 20–25 wt.% of silica. Rice husk is usually discarded and burned in the fields. This common practice can lead to serious environmental damage, since silica particles remain suspended in the air being a potential cause of respiratory diseases. In Brazil, for example, about 2.5×10^6 tonnes of rice hull ash (RHA) are generated each year [9]. RHA is a black residue which contains approximately 85–90 wt.% of silica, 10–15 wt.% of carbon, small amounts of alkalis and other trace elements [10].

As the world production of rice hulls (RHs) is estimated to be 80 million tonnes annually, which corresponds to ~3.2 million tonnes of silica [11], it seems a reasonable assumption that this agricultural waste presents great potential use in large scale, such as in ceramic, cement and composite industries. Indeed, RH has been used as raw materials for the production of a series of silicon-based materials, including silicon carbide [12,13], silica [14], silicon nitride [15], reinforced polymer composites [16], cements [9] and other silicon-based materials [17].

Concerning the above ideas, the motivation of this work was to produce ceramic matrix composites (CMCs) derived from a polysiloxane network using rice husk ash as the reactive filler. Such an approach associates the advantages offered by the polymeric precursor route in the production of CMCs and also draws attention to a novel way to consume the RHA, and therefore, contributes to new applications of this agricultural waste. RHA-filled polysiloxane was prepared by mixing the RHA powder with the liquid precursor, forming the polysiloxane network (PN) through a hydrosilylation reaction *in situ*. Such PN have already been studied and found to produce at 1000 °C, a silicon oxycarbide glass with high amount of carbidic groups as well as a free carbon phase [4]. The pyrolysis of the RSH-filled PN was carried out up to 1000 and 1600 °C, in an argon atmosphere, giving rise to novel ceramic matrix composites. These composites were characterized by thermogravimetric (TGA) and thermal differential (DTA) analyses, X-ray diffraction (XRD), scanning electron microscopy (SEM) with energy-dispersive X-ray spectroscopy (EDS), in addition to density and mechanical measurements. The effect of three polymeric infiltration cycles on the morphological and mechanical properties of the resulting CMCs obtained at 1000 °C was also studied.

2. Experimental procedures

2.1. Sample preparation

The rice husk (RH) *in natura* was obtained from Nazareno, a city located in Minas Gerais state, in Brazil. It was washed with water and H_2SO_4 solution (1%, v/v) under vigorous stirring for 30 min. After which it was washed with distilled water until reaching a neutral pH. The RH was dried at 60 °C for 48 h. Rice husk ashes (RHAs) were obtained by pyrolysis of the RHs in a muffle oven under an oxidant (environmental) atmosphere while heating up to 400 °C, at 10 °C/min, and held at this temperature for 30 min.

A polysiloxane network, PN, used as a preceramic polymer, was prepared according to [4]. The preparation involved *in situ* hydrosilylation reaction between the 1,3,5,7-tetramethyl-1,3,5,7-tetravinylcyclotetrasiloxane (D_4Vi) and poly(methylsiloxane) (PMHS) with an average molecular weight of 2300 g/mol and viscosity of 30 cst (both from Dow Corning), in a 1:1 weight ratio, using a platinum divinylcomplex, 2–3% in vinyl-terminated poly(dimethylsiloxane) (Pt-catalyst) (Hülls), and in a 1% in relation to the total mass. The mixture was previously homogenized by magnetic stirring for 90 min.

Green bodies of RHA/polysiloxane network were prepared by blending the RHA with the D_4Vi, PMHS and Pt-catalyst mixture (liquid precursor) in a weight ratio of 4:1, respectively. The mixture was compacted in a steel mold (100 mm × 5 mm × 3 mm) of stainless steel and the stabilization of the green bodies was achieved by a thermal cross-linking reaction at 70 °C, over a period of 2 h.

Pyrolysis of the monolithic compacts was carried out in a tube furnace—Edgcon 10P or in a Thermolyne F59340-CM (for temperatures at 1600 °C), both of which were equipped with an internal alumina tube, under either argon or nitrogen flow (~100 mL/min), in a step-heating schedule. The heating cycle involved heating to 1000 or 1600 °C, at 5 °C/min, holding at the final temperature for 60 min. Then, the samples were cooled down to room temperature, at 2 °C/min. All the experiments yielded monolithic and crack-free samples.

Infiltration cycles were carried out in the CMCs obtained at 1000 °C. CMCs were immersed in the liquid precursor, and the system was maintained under vacuum for 10 min. After that, the system was kept at room temperature until completely cured. The excess polymer was removed and the composite was pyrolised at 1000 °C as described before. This process was repeated twice.

2.2. Sample characterization techniques

Absolute densities were measured with a helium pycnometer (Micromeritics, model 1035) and the bulk densities were calculated by the ratio of mass over volume for suitable rectangular bars. Open porosity was determined by the ratio of bulk/absolute density values.

Thermogravimetric analysis was performed on a thermobalance (2950, TA Instruments) and differential thermal analysis was performed on a calorimeter (TA Instrument, model 2910). Both analyses were performed under flowing argon or synthetic air (100 mL/min), with a heating rate of 10 °C/min until the maximum temperature was reached.

The carbon content in the RHAs was analyzed by elemental analysis (PerkinElmer, model 2400), using the standard procedure described in the literature [18].

X-ray diffraction patterns were collected with a diffractometer (Shimadzu, model XD3A) using Cu Kα radiation ($\lambda = 0.15418$ nm) as the incident beam.

Microstructural characterization was performed by scanning electron microscopy (LEO 435VPI and JEOL-JSM 6360LV), operating with an accelerating voltage of 20 kV. The last instrument is also equipped with an energy-dispersive X-ray

spectroscopy Be-detector (Noran Instruments) allowing chemical analysis. For SEM analysis, samples were previously covered with a thin Au layer, by using a sputtering equipment (BAL-TEC 020). For EDS analyses a graphite sample holder was used, and the samples were not covered.

Mechanical properties of CMCs were measured by four-point bending tests using an Instron Universal Testing Machine with a crosshead speed of 0.5 mm min^{-1} with a space:thickness ratio of 30:1, which is in agreement with ASTM (1161-94—Standard Test Method for Flexural Strength for Advanced Ceramics at Ambient Temperature).

3. Results and discussion

3.1. Characterization of RHA

TG and DTG curves of RH sample on both inert and oxidant atmospheres up to 1000 °C are displayed in Fig. 1. The initial step of weight loss, which started at 50 °C for both atmospheres, was associated with the evolution of residual physically adsorbed water corresponding to ~6 wt.%. The weight loss associated with the RH pyrolytic process started at ~230 °C for both atmospheres and finished at ~520 and ~800 °C for the analysis in oxidant and inert atmospheres, respectively. This main degradation process occurred in three steps of weight losses. The temperature of maximum degradation, T_{MAX}, of each step was 303, 329 and 449 °C for analysis under oxidant atmosphere. For the analysis in argon atmosphere, the T_{MAX} of each step was, 320 and 358 °C for the first and second degradation steps, and just a lump was observed for the third step. These three degradation steps were related to the thermal degradation of hemicellulose, cellulose and lignin, respectively [19]. As the third degradation step for the sample pyrolysed under the inert atmosphere was actually not an obvious peak in the DTG curve but was more like a gentle sloping baseline, the lignin degradation in this condition was much slower than that one observed in oxidant atmosphere. This result is in accordance with previous findings [19,20]. Indeed, while the residue obtained under oxidant pyrolysis was white, the residue obtained at inert atmosphere was black, probably due to the presence of carbon char from the incomplete lignin degradation. However, the char yields at 1000 °C, after which both samples were the same, 11.1 wt.%.

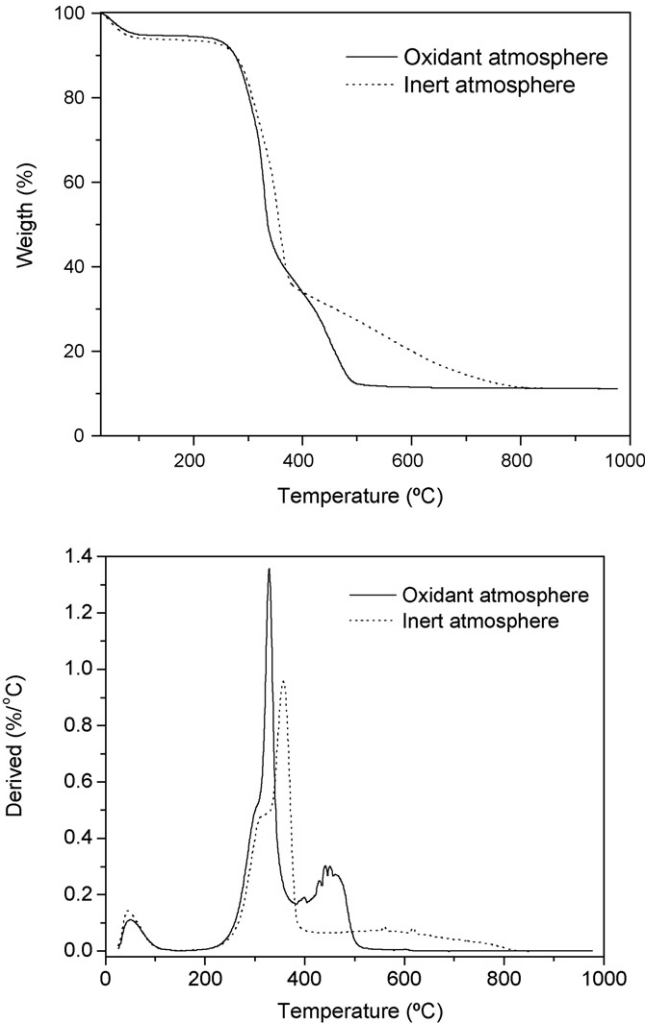

Fig. 1. TG and DTG curves recorded during pyrolysis of RH under inert and oxidant atmospheres (10 °C/min).

The residues of the RHs treated under oxidant and inert atmospheres at 400 °C were also analyzed. Although the char yields at this temperature were similar for both samples (33.8 and 34 wt.%, respectively), the carbon content, determined by elemental analysis, was quite different (47.1 and 56.7 wt.% for the samples obtained at oxidant and inert atmosphere, respectively). Thus, it was established that the best composition for the RHA to act as a reactive filler in polysiloxane matrix would be the one obtained from the oxidant atmosphere, at 400 °C.

Fig. 2 shows a SEM micrograph of the RHA obtained under inert atmosphere (Ar) at 1000 °C, in addition to energy-dispersive X-ray spectra of two selected areas. It was possible to observe the formation of longer and thin particles, with a morphology derived from the organic structures in the image. Such kinds of particles have already been explored in the literature to be high potential materials for obtaining mullite whiskers at higher temperatures [11]. EDS analysis of the internal and external surfaces of some analyzed particles indicated some heterogeneity regarding the silica and carbon phases. The internal surface showed much higher amounts of carbon than the external surface, which showed silicon as the major constituent. This observation can be justified from an evolutive process, where silicon is present in large concentration as in silica, mainly in the protuberances, thricomes and in the external epidermis, promoting higher mechanical resistance for the RHs and provides subsequent protection to the grains [21].

Fig. 3 shows the XRD patterns of RHA treated under inert and oxidant atmospheres at different temperatures. The samples obtained under an inert atmosphere at 600 and 1000 °C are amorphous. Their XRD spectra show only one main halo around 22° (2θ), typical of amorphous silica-based glasses. A similar pattern was observed for the sample obtained under an oxidant atmosphere at 400 °C. However, in addition to the main

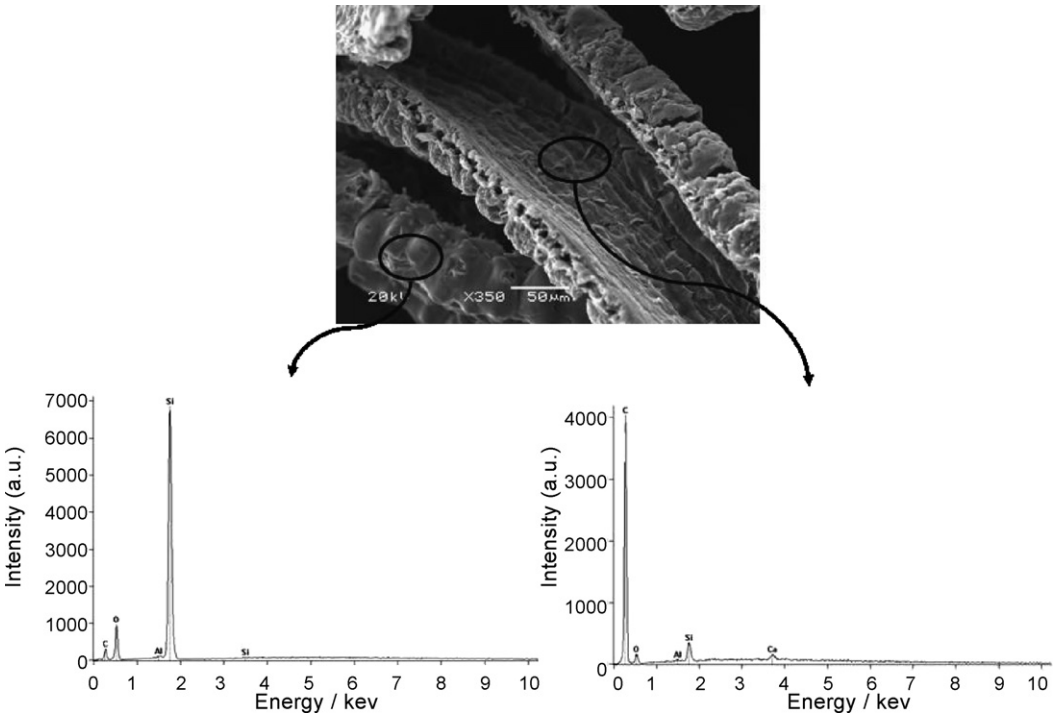

Fig. 2. SEM micrograph of the inner and outer surfaces of the RHA pyrolysed at 1000 °C in an argon atmosphere with the corresponding energy-dispersive X-ray spectroscopy (EDS) of the selected areas.

halo around 22° (2θ), samples obtained at 1000 °C showed further crystalline peaks at 20.85°, 26.66°, 36.56°, 39.49° and 50.21° (2θ), which were assigned to hexagonal α-quartzo, while the peaks at 21.58° were assigned to the onset crystallization of trydimite phase.

XRD spectra have also been collected on samples pyrolysed under an argon atmosphere at 1300 and 1600 °C, as can be seen in Fig. 4. Besides the halo around 22° (2θ), the XRD spectra recorded on the sample obtained at 1300 °C shows crystalline peaks at 21.8°, 36° and 60° (2θ), which were assigned to the onset crystallization of trydimite. On the other side, the diffraction peaks of hexagonal 6H–SiC at 35.8°, 65.2° and 71.7° (2θ) and 2H–SiC at 33.6°, 37.7° and 49.5°(2θ) were observed at 1600 °C. The formation of these crystalline phases of SiC resulted from the carbothermal reduction reaction of the silica, according to the equation below (Eq. (1)) [12,22]. It is important to notice that although the carbothermal reaction is very active above 1450 °C, the slight halo centered at 23° (2θ) in the XRD pattern evidences that the reaction was not completed. It is a reasonable assumption that the residual carbon amount was not sufficient for the complete reaction to take place.

$$SiO_{2(s)} + 3\,C_{(s)} \rightarrow SiC_{(s)} + 2CO_{(g)} \quad (1)$$

3.2. Characterization of the green body

SEM observations performed on the surface fracture of the green body (not shown) evidenced a homogenous dispersion of the PN polymer on the RHA particles. The well-dispersed and continuous polymeric phase on the powder surface is easily achieved due to the low viscosity and surface tension of the siloxane precursors. PN polymer was prepared via a hydrosilylation reaction, which occurs between the Si–H, from PMHS, and Si–CH=CH_2, from D_4Vi, in the presence of Pt^{II} catalyst. According to the reaction scheme shown in Fig. 5, no by-product is formed in this reaction [23].

The PN is a silicone network and its structural evolution to ceramic material was already fully investigated by ^{29}Si and ^{13}C MAS NMR, XRD and TGA techniques [4]. The hydrosilylation reaction enables it to incorporate more than 70% of reactive functions in the polysiloxane network, resulting in a high cross-linking density precursor, making it useful for the CMC forming technology. PN is an excellent precursor of SiOC, with 70% of ceramic yield at 1000 °C. In relation to Si sites distribution, this amorphous ceramic presents the following composition: SiO_4 (25%), SiO_3C (30%), SiC_2O_2 (21%) and SiC_3O (24%) [4]. The amount of rich-carbidic sites such as SiC_4 and SiO_2C_2 is higher than those usually observed in glass products obtained from the pyrolysis of alkoxysilane gels reported in literature, which consist primarily of SiO_4, SiO_3C [5]. The residual carbon content (free carbon) estimated by elemental analysis was 70 wt.% (in relation to the total carbon).

3.3. Characterization of CMC

Fig. 6 presents TG and DTG curves of the PS and green body samples recorded on an argon atmosphere. The green body showed an initial weight loss process, with ∼5 wt.%, probably due to the volatilization of residual water (from RHA) and D_4Vi oligomers not incorporated to polysiloxane network. It is a

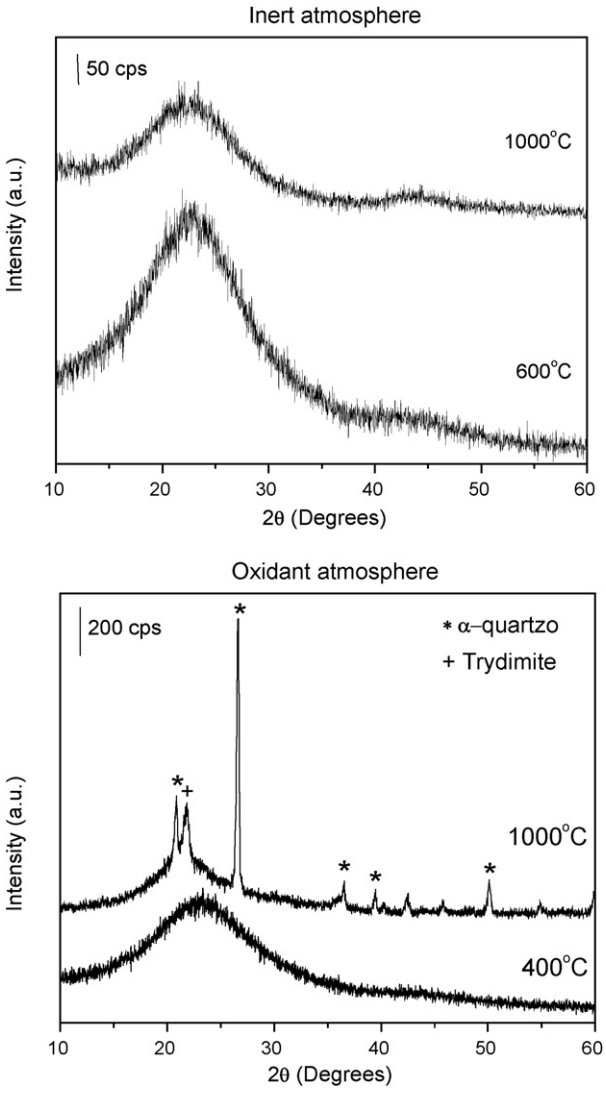

Fig. 3. XRD patterns of the RHAs treated under different atmospheres and temperatures.

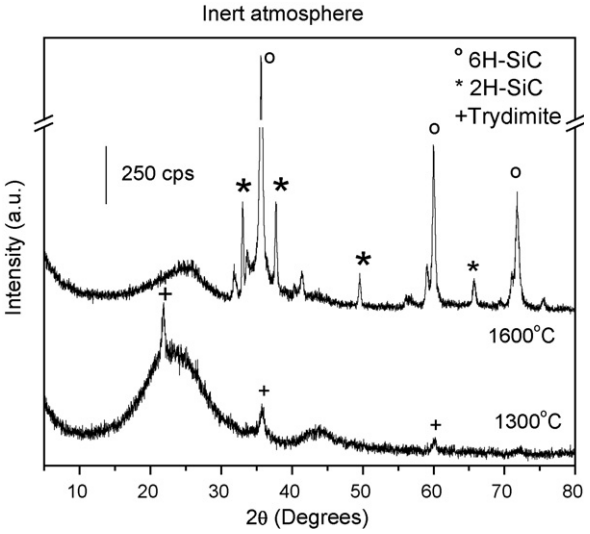

Fig. 4. XRD patterns of the RHAs pyrolysed at 1300 and 1600 °C under an inert atmosphere.

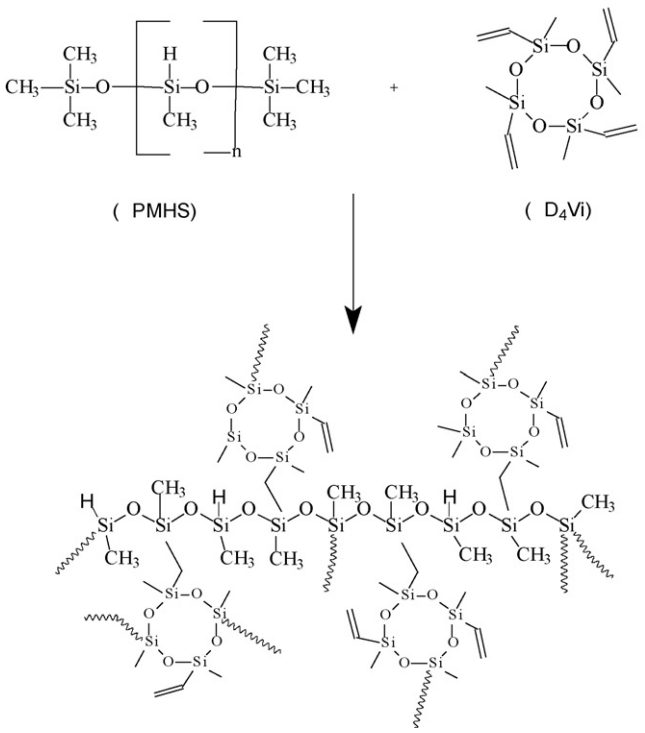

Fig. 5. Schematic reaction between the D_4Vi oligomer and PMHS homopolymer giving rise to the polysiloxane network (PN) precursor.

reasonable assumption that the filled polymer has a lower cross-linking degree, and at this temperature range, it is not expected reactions between polymeric network and reactive filler as well. The second weight loss process (from ~400 up to 900 °C) in the DTG curves for PN and green body are formed by at least two overlapped steps of the degradation process. T_{MAX} for the first and second steps were 622 and 720 °C for the PN sample, and 575° and 695° for the green body sample, respectively. Such degradation steps are related to the polymer-to-ceramic conversion [4,5]. As the curves displayed similar profiles, it is reasonable to assume that no significant reaction between the PN or PN degradation products with the RHA occurred, up to

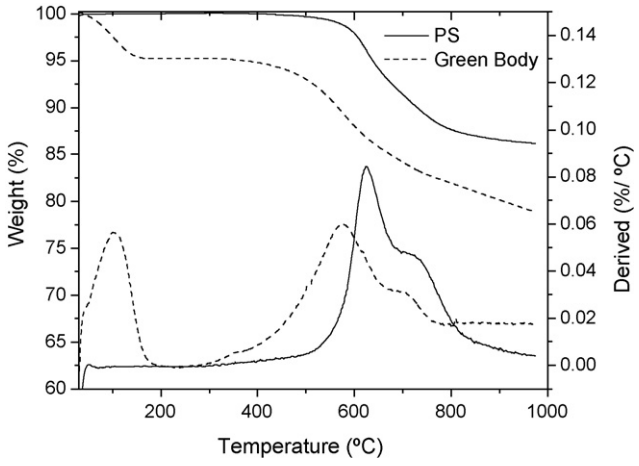

Fig. 6. TG and DTG curves recorded during pyrolysis of PN and green body under argon atmosphere (10 °C/min).

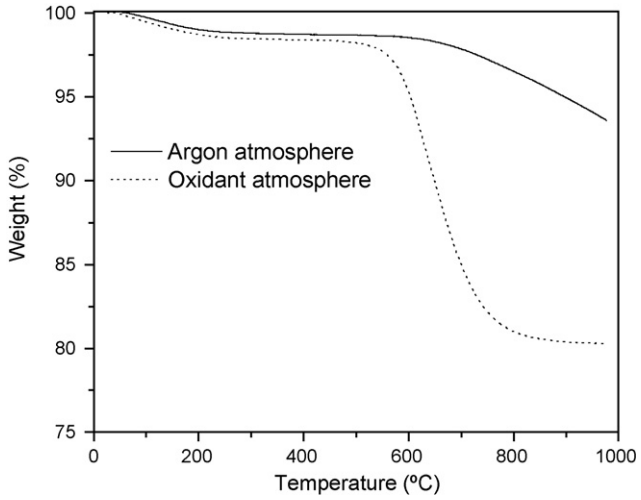

Fig. 7. TG curves recorded under inert and oxidant atmospheres of the CMC obtained at 1000 °C (10 °C/min).

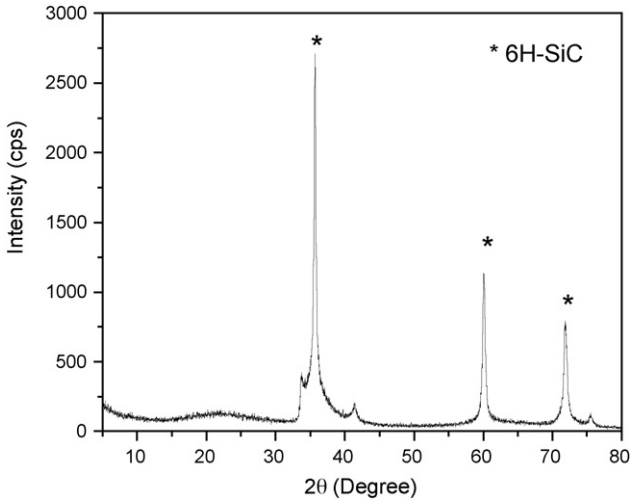

Fig. 8. XRD pattern of the CMC obtained at 1600 °C under inert atmosphere.

the temperature analyzed. This means that up to 1000 °C, the RHA acted as an inert filler. The ceramic yields taken from the TG curves, for the PN and green bodies, were 86.1 and 78.8 wt.%, respectively.

In order to verify the thermal stability of the CMC obtained at 1000 °C, TG analyses were recorded on these samples under both inert and oxidant atmosphere, as can be seen in Fig. 7. CMC treated under an inert atmosphere showed higher thermal stability up to temperatures around 700 °C, with a loss of 5 wt.% in a continuous process up to 1000 °C. On the other side, the curve showed a significant loss of 20 wt.% up to 1000 °C under oxidant atmospheres. This weight loss can be related to the residual-free carbon from the RHA filler. Consequently, a lower stability of the CMC under oxidant atmosphere was observed when compared to the same treatment under argon atmosphere.

X-ray pattern of the CMC obtained at 1000 °C (not shown) was characteristic of an amorphous material, while that obtained at 1600 °C (Fig. 8) showed diffraction peaks of 6H–SiC, suggesting that carbothermal reduction reaction was

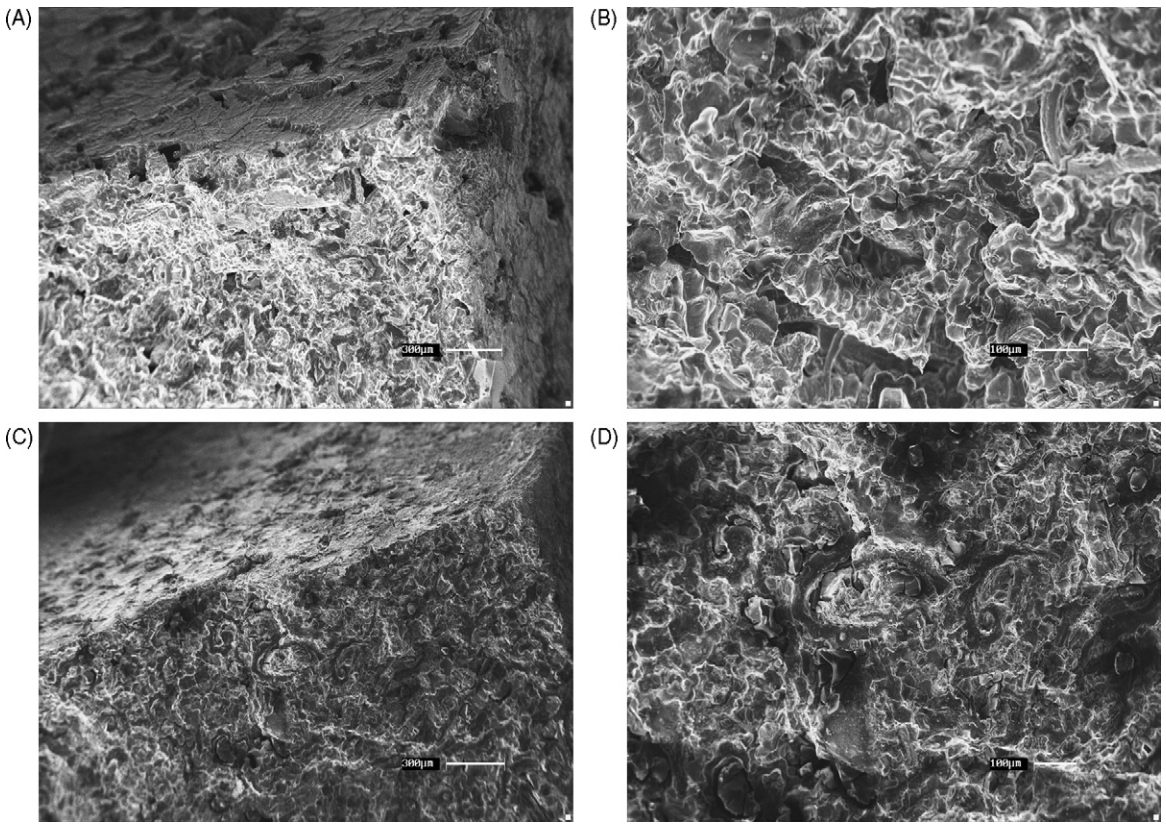

Fig. 9. SEM micrographs of the fracture surface of the CMCs obtained at 1000 °C in an argon atmosphere before (A and B) and after one infiltration cycle (C and D).

Table 1
Bulk and absolute densities and open porosity values for the green bodies and CMCs obtained at 1000 °C before and after infiltration

Sample	Bulk density (g/cm^3)	Absolute density (g/cm^3)	Open porosity (%)
Green body	0.93 ± 0.02	–	–
CMC 1000 °C	1.29 ± 0.02	1.98 ± 0.01	34.7
CMC 1000 °C 1st infiltration	1.51 ± 0.02	1.88 ± 0.01	19.8
CMC 1000 °C 2nd infiltration	1.67 ± 0.02	1.94 ± 0.01	14.1

Table 2
Mechanical properties of the ceramic composites obtained at 1000 °C before and after infiltration

CMC Sample	Flexural strength (MPa)	Flexural modulus (GPa)
CMC 1000 °C	10.6 ± 2.6	11.1 ± 2.3
CMC 1000 °C 1st infiltration	14.9 ± 1.7	15.0 ± 1.6
CMC 1000 °C 2nd infiltration	21.7 ± 2.1	23.5 ± 2.6

complete. These results confirm the large potential of the RHAs to act as reactive filler in a polysiloxane network at higher temperatures, since the polymer-derived ceramic can supply the carbon amount for complete carbothermal reduction to take place.

Bulk and absolute densities of the CMC obtained at 1000 °C were 1.29 and 1.98 g/cm^3, respectively. These values give an open porosity of 34.7% (Table 1). This porosity was due to the partial filling of the pores by the PN preceramic polymer as well as the agglomeration of irregular shape filler particles. SEM observations performed on the surface fracture of the CMC showed a homogenous dispersion of the PN-derived ceramic phase on the RHA particles, as can be seen in Fig. 9A and B. Although this high porosity value is generally observed for the CMCs prepared from the polymer route [3,8], such an approach can also offer a simple way to reduce the porosity by polymer infiltration cycles [4]. In order to decrease the porosity observed in the CMC obtained by pyrolysis at 1000 °C, and get more insight about the role of the polymeric precursor in the microstructure and properties of the final CMCs, infiltration cycles of the polymeric precursor still in the liquid form were carried out. Table 1 presents the bulk and absolute density values and the open porosity of the green body and the CMC obtained at 1000 °C before and after two infiltration cycles. The increase of initial bulk density from the green body to the CMC was due to the organic-to-inorganic conversion of the polymer precursor to a silicon oxycarbide glass [3,6]. From Table 1 data, it can be observed that while the bulk density increased with the infiltration cycles due to filling up of the voids in the structure of the ceramic bodies by the polymer-derived ceramic, the absolute density only slightly changed. The result of this microstructure change is the decrease of the open porosity.

Fig. 9 displays SEM micrographs of the fracture surface of the CMCs obtained at 1000 °C in an argon atmosphere before (A and B) and after one infiltration cycle (C and D). The samples submitted to the infiltration process presented a more dense morphology. In spite of the high porosity observed in the CMC before infiltrations, the main advantage offered by the polymer-derived ceramic route is the possibility to perform infiltration cycles to achieve an expected density.

Table 2 presents the mechanical property values of the ceramic composites obtained at 1000 °C before and after the infiltration cycles. The CMCs presented brittle fracture and the flexural strength and modulus values were relatively low as expected for ceramic composites. Such results are in accordance with other data involving polymer-derived ceramic composites [24]. However, the mechanical properties increased 50% after one infiltration cycle and 100% after two infiltration cycles, indicating that the polymer precursor route was appropriate to improve the mechanical and microstructure properties of CMC.

4. Conclusions

In this study, it was possible to observe the great potential of RHA as reactive filler for obtaining CMCs through pyrolysis of silicon-based polymer composites, generating uniform materials without macroscopic defects or cracks based in SiOC or SiC. In spite of the porosity observed, CMC with good mechanical properties was obtained. For the reduction of the porosity observed, infiltration cycles of the polymeric precursor were successfully carried out, resulting in CMCs with lower porosity and higher flexural strength and modulus values. In conclusion, besides the economical benefits in the usage of this wasted material, the methodology used here seems to be an attractive alternative method for obtaining of ceramic matrix composites with a variety of potential applications.

Acknowledgements

We gratefully acknowledge financial support from FAPEMIG (Grant CEX-925/04) and CNPq (Grant 478563/04-3).

References

[1] R. Riedel, G. Mera, R. Hauser, A. Klonczynsky, Silicon-based polymer-derived ceramics: synthesis properties and applications—a review, J. Ceram. Soc. Jpn. 114 (6) (2006) 425.
[2] M.A. Schiavon, S.A.U. Redondo, S.R.O. Pina, I.V.P. Yoshida, Investigation on kinetics of thermal decomposition in polysiloxane networks used as precursors of silicon oxycarbide glasses, J. Non-Cryst. Solids 304 (2002) 92–100.
[3] M.A. Schiavon, E. Radovanovic, I.V.P. Yoshida, Microstructural characterisation of monolithic ceramic matrix composites from polysiloxane and SiC powder, Powder Technol. 123 (2002) 232–241.
[4] E. Radovanovic, M.F. Gozzi, M.C. Gonçalves, I.V.P. Yoshida, Silicon oxycarbide glasses from silicone networks, J. Non-Cryst. Solids 248 (1999) 37–48.
[5] C.G. Pantano, A.K. Sing, H. Zhang, Silicon oxycarbide glasses, J. Sol–Gel Sci. Technol. 14 (7) (1999) 7–25.
[6] P. Greil, Active-filler-controlled pyrolysis of preceramic polymers, J. Am. Ceram. Soc. 78 (4) (1995) 835–848.
[7] P. Greil, M. Seilbold, Modeling of dimensional changes during polymer ceramic conversion for bulk component fabrication, J. Mater. Sci. 27 (1992) 1053–1060.

[8] M.A. Schiavon, I.V.P. Yoshida, Ceramic matrix composites derived from $CrSi_2$-filled silicone polycyclic network, J. Mater. Sci. 39 (2004) 4507–4514.
[9] F.A. Rodrigues, Low-temperature synthesis of cements from rice hull ash, Cement Concrete Res. 33 (2003) 1525–1529.
[10] R.V. Krishnarao, Y.R. Mahajan, Effect of acid treatment on the formation of SiC whiskers from raw rice husks, J. Eur. Ceram. Soc. 15 (1995) 1229–1234.
[11] M.F. de Souza, P.S. Batista, I. Regiani, J.B.L. Liborio, D.P.F. de Souza, Rice hull-derived silica: applications in Portland cement and Mullite whiskers, Mater. Res. 3 (2) (2000) 25–30.
[12] K. Sujirote, P. Leangsuwan, Silicon carbide formation from pretreated rice husks, J. Mater. Sci. 38 (2003) 4739–4744.
[13] V. Martinez, M.F. Valencia, J. Cruz, J.M. Mejía, F. Chejne, Production of β-SiC by pyrolysis of rice husk in gas furnaces, Ceram. Int. 32 (2006) 891–897.
[14] S. Chandrasekhar, K.G. Satyanarayama, P.N. Pramada, P. Raghavan, T.N. Gupta, Processing, properties and applications of reactive silica from rice husk—an overview, J. Mater. Sci. 38 (2003) 3159–3168.
[15] C. Real, D.M. Alcalá, J.M. Criado, Synthesis of silicon nitride from carbothermal reduction of rice husks by the constant-rate-thermal-analysis (CRTA) method, J. Am. Ceram. Soc. 87 (1) (2004) 75–78.
[16] H. Unuma, K. Niino, K. Sasaki, Y. Shibata, H. Iizuka, S. Shikano, T. Nakamura, Preparation and characterization of glass-like carbon/silica composites from rice hull and phenolic resin, J. Mater. Sci. 41 (2006) 5593–5597.
[17] L. Sun, K. Gong, Silicon-based materials from rice husks and their applications, Ind. Eng. Chem. Res. 40 (2001) 5861–5877.
[18] P.P. Borda, P. Legzdins, Determination of carbon content in carbides by Na elemental analyser, Anal. Chem. 52 (1980) 1777.
[19] H. Teng, H.-C. Lin, J.-A. Ho, Thermogravimetirc analysis on global mass loss kinetics of rice hull pyrolysis, Ind. Eng. Chem. Res. 36 (1997) 3974–3977.
[20] M.J. Antal, G. Varhegy, Cellulose pyrolysis kinetics—the current state knowledge, Ind. Eng. Chem. Res. 34 (1995) 703–717.
[21] E. Natarajan, A. Nordin, A.N. Rao, Overview of combustion and gasification of rice husk in fluidized bed reactors, Biomass Bioenerg. 14 (1998) 533–546.
[22] D.H. Filsingeril, S.A. Jansson, Silica to silicon: key carbothermic reactions and kinetics, J. Am. Ceram. Soc. 73 (6) (1990) 1726–1732.
[23] M.J. Michalczyk, E.E. Farneth, A.J. Vega, High-temperature stabilization of cross-linked siloxanes glasses, Chem. Mater. 5 (1993) 1687–1689.
[24] M.A. Schiavon, L.C. Pardini, I.V.P. Yoshida, Processing of monolithic ceramic bodies from polysiloxane precursor, Key Eng. Mater. 189 (2001) 48–53.